SECULAR WARMING IN THE CALIFORNIA CURRENT AND NORTH PACIFIC

DAVID FIELD
Monterey Bay Aquarium Research Institute
7700 Sandholdt Road
Moss Landing, California 95039
dfield@mbari.org

DAN CAYAN
Scripps Institution of Oceanography
University of California, San Diego
La Jolla, California 92093-0227

FRANCISCO CHAVEZ
Monterey Bay Aquarium Research Institute
7700 Sandholdt Road
Moss Landing, California 95039

ABSTRACT

The role of secular warming relative to decadal and spatial variability in ocean temperature is examined from long-term Sea Surface Temperature (SST) records off California, from other regions of the North Pacific, and from the Indian Ocean. The Pacific Decadal Oscillation (PDO) index of basin-scale variability accounts for 18–48% of the variability in these SST series. The warming trend in SST is now associated with similar levels of variability. Near-surface temperature variations throughout the California Current System are similar between regions, including the waters over the Santa Barbara Basin. Changes in the abundances of planktonic foraminifera from Santa Barbara Basin sediments show that the warming trend has had a substantial impact on marine populations relative to other interannual- to decadal-scale changes. Time series that began after 1925 may underestimate the cold extremes of decadal-scale ocean variability and its modulation of marine populations while records since 1977 lie within an anomalously warm period.

INTRODUCTION

Long-term warming of the world's oceans and its effects on marine ecosystems are currently major concerns and are widely debated. The integrated heat content of the global oceans to 3000 m has been increasing since the mid-1950s and observations and models show that the increases can be attributed to atmospheric forcing associated with accumulating greenhouse gasses in the atmosphere (Levitus et al. 2000; 2001; Barnett et al. 2001; 2005). Many coral records from the tropical Pacific and Indian Oceans show unprecedented warming in the late 20th century (Urban et al. 2000; Charles et al. 2003; Cobb et al. 2003). Moreover, fossils from marine sediments indicate that recent warming in the California Current System (CCS) has affected marine populations in a manner that is different from warming events during the previous 1400 years (Field et al. 2006). In this study, SST time series from the CCS and other regions of the North Pacific are analyzed to show the nature of the warming trend relative to decadal variability.

Changes in ocean-atmosphere heat exchange, horizontal advection, vertical mixing, and wind-driven shoaling and deepening of the thermocline are important processes that affect SST and redistribute heat within the ocean and between the ocean and atmosphere on seasonal to millenial time scales. It is well known that the CCS and the North Pacific undergo large interannual- (El Niño Southern Oscillation [ENSO]) and decadal-scale variations that can be largely characterized by the North Pacific Index (NPI; Trenberth and Hurrell, 1994) of atmospheric circulation and the Pacific Decadal Oscillation (PDO) index of SST. The cause of this decadal-scale variability is likely related to a combination of oceanic integration of white noise weather, tropical forcing, and mid-latitude feedbacks (Pierce 2001; Rudnick and Davis 2003; Deser et al. 2004; Miller et al. 1994; Schneider and Cornuelle 2005). Enfield and Mestas-Nuñez (1999) showed that in addition to large interannual and decadal variability, the eastern North Pacific makes an important contribution to the global ocean warming trend that began around 1930 and further intensified in the mid-1970s.

The PDO is often employed instead of regional temperature records or atmospheric indices as an indicator of the state of North Pacific climate because it integrates the oceanic response to large-scale processes. In addition, uncertainty in the reliability of both the PDO and regional records in the early 20th century arises from a fairly limited number of observations in the Comprehensive Oceanic-Atmospheric Data Set (COADS) and potential biases in methodology, although these have been well described (Kaplan et al. 1998; Lluch-Belda et al. 2001; Smith and Reynolds 2004). By definition, the PDO is the dominant pattern of variability in SST in the North Pacific; it is the leading principal component of Pacific Ocean SSTs north of 20°N and primarily captures a dipole of anomalous SSTs between the central and the eastern North Pacific (fig. 1). However, the PDO is calculated after removing the mean monthly global SST anomaly, which has an appreciable upward trend (approximately +0.6°C since 1900). Various studies (Mantua et al. 1997; Deser et al. 2004; Schneider and Cornuelle, 2005) have examined the mechanisms responsible for the variability associated with the PDO, but not the trend. Although it is generally known that

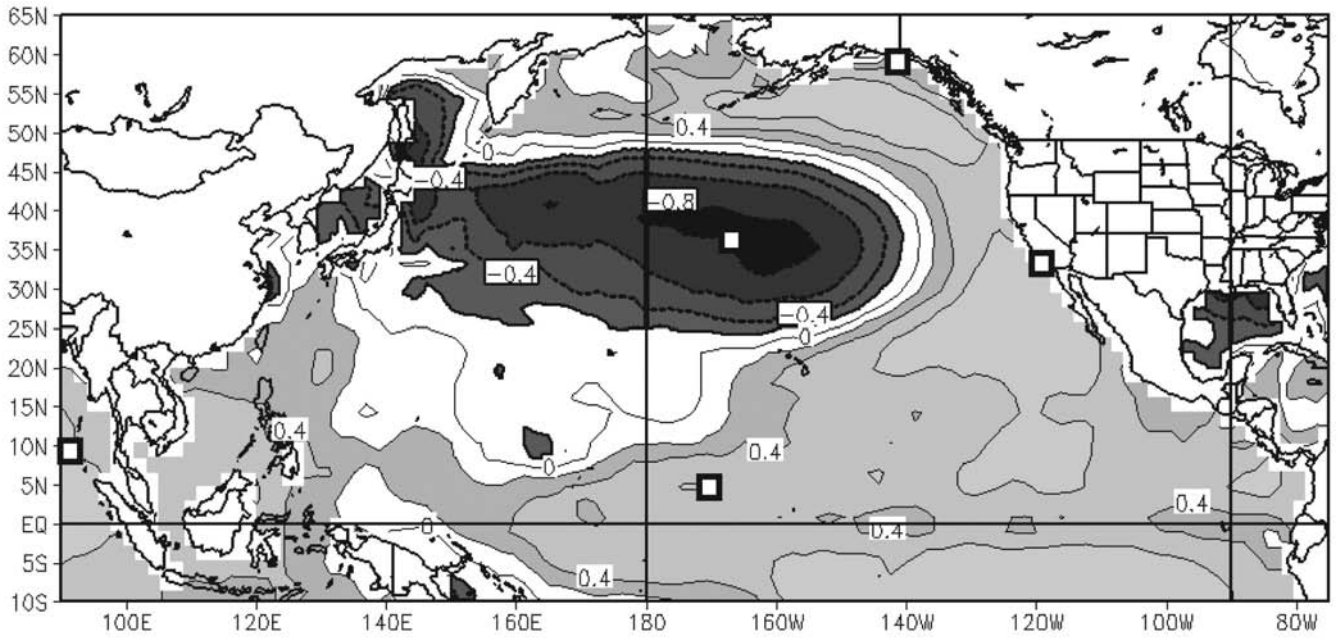

Figure 1. Correlation of SSTs with the PDO index from 1948–2003 illustrating the general spatial pattern of SST anomalies associated with the PDO. Squares indicate locations of SST series used in this study (California Current records are shown in fig. 2).

the trend is not included in the PDO, the relative effects of the warming trend on ocean climate and marine population response may be frequently overlooked.

Some of the longest biological time series available are commercial fish catch records, which indicate that decadal variability associated with the PDO has a predominant effect on many marine populations (Mantua et al. 1997; Chavez et al. 2003). Sedimentary records of fish scale deposition suggest that the decadal variations of the 20th century are typical of population variability prior to fishing (Baumgartner et al. 1992). While anthropogenic effects of fishing at multiple trophic levels (prey and predator) must have some influences, it is difficult to separate the effects of removal from responses to secular changes in climate. Other studies have attributed recent changes in marine populations to the 20th century warming trend (Barry et al. 1995; Field et al. 2006), but few studies have discussed the relative importance of both the PDO and the trend to marine populations.

We quantify the variance associated with the PDO and with the warming trend. In order to show how well time series of a given location, duration, and sampling resolution reflect these two sources of large-scale variability, we examine time series of SST from shore stations as well as shipboard measurements from COADS and California Cooperative Oceanic and Fisheries Investigations (CalCOFI). Links between SST variability and the trend on marine populations in the CCS are illustrated by presenting records of abundance of different species of planktonic foraminifera from Santa Barbara Basin sediments that span >250 years as described by Field et al. (2006) and Field (2004a). Using a sequence of these foraminiferal variations, changes in spatial patterns of Pacific SSTs are examined and the scale and physical mechanisms of change that may be affecting the North Pacific and its ecosystems are discussed.

MATERIALS AND METHODS

SST time series selected for this study are Scripps Pier in La Jolla and Pacific Grove near Monterey (fig. 2), both of which span two decadal-scale fluctuations of the PDO index. Two common COADS-derived SST indices off of southern/central California were selected: the Kaplan SST index at the 5° × 5° grid centered 32.5°N and 122.5°W (Kaplan et al. 1998), and the Extended Reconstructed SST (ERSST) at the 2° × 2° grid located at 34°N and 118°W (Smith and Reynolds 2004). These locations, shown in Figure 2, were selected for multiple reasons. First, the variations in SST in the CCS show the strongest relationship with the PDO off southern California (fig. 1). Additionally, examination of gridded ship- and buoy-observed SST off of southern and central California allows direct comparison with SST records from Scripps Pier, the longest shore station available, and from the Santa Barbara Basin, the location of high resolution sedimentary records extending further back in time. Also, CalCOFI sampling in this region since 1950 permits additional examination of spatial patterns of variability. ERSST indices from three other locations around the North Pacific and one location in the Indian Ocean were also selected to examine a range of areas that show a strong relationship with the PDO (fig. 1).

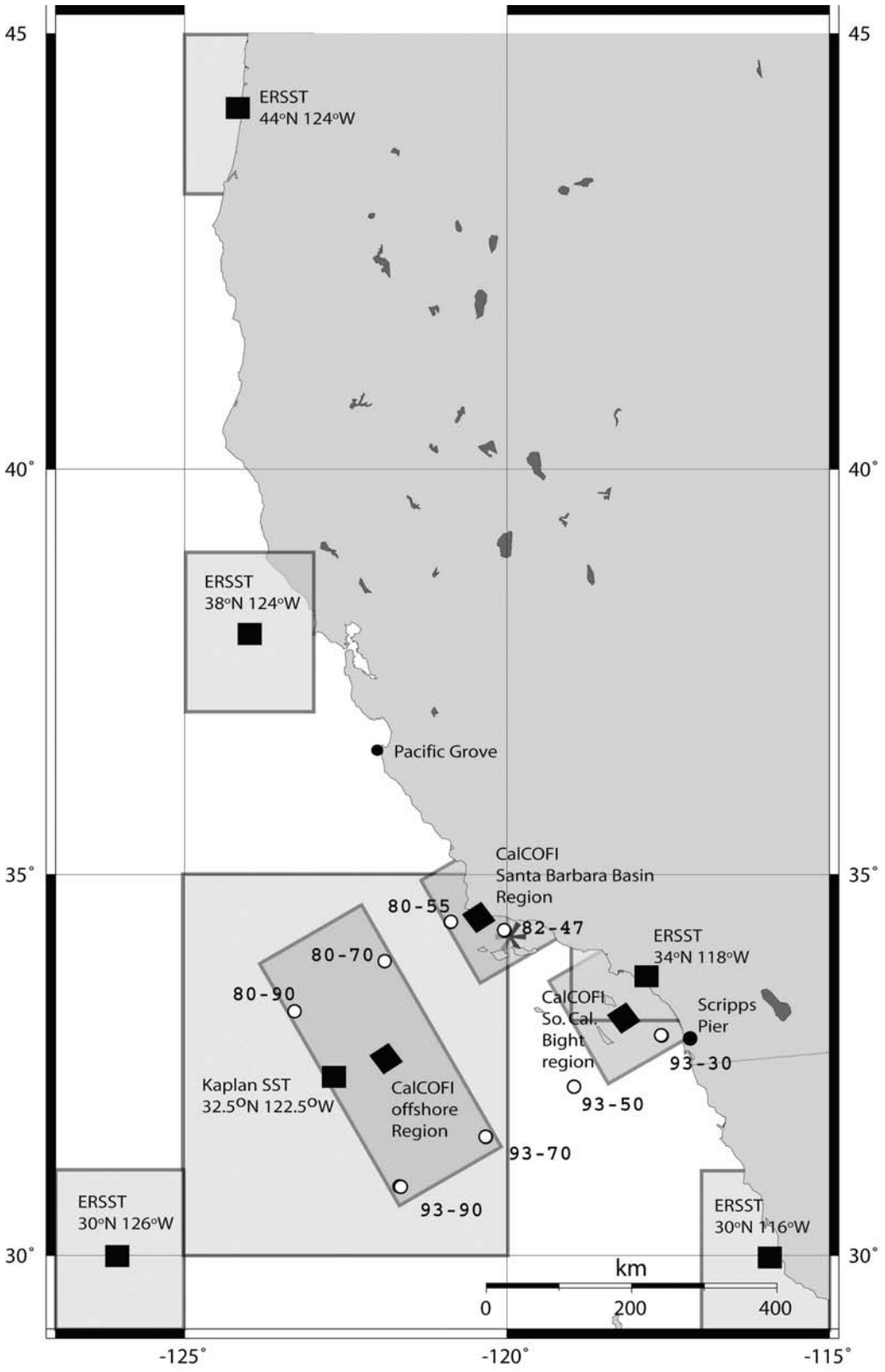

Figure 2. Map of the California Current showing locations of time series used in this study from shore stations at Pacific Grove and Scripps Pier (bold circles), the location of the Santa Barbara Basin(*), select CalCOFI stations used to examine variability with individual stations (open circles), the CalCOFI grids encompassing other stations used to calculate a CalCOFI grid average (slanted boxes), the Kaplan SST index of the 5° × 5° grid centered at 32.5°N and 122.5°W, and five different 2° × 2° ERSST grids.

TABLE 1

Coefficients of determination (r^2 values) for the trend in the SST series shown in Figures 3B–I (data) and 3K–R (residuals of those data from the PDO). Bold values indicate significance at $p < 0.05$ after correcting for multiple testing. Also shown are the standard deviations and range of each series, as well as the regression coefficients of the slope of the residuals that indicate the rate of warming (per year). For comparison, the trend in average global SST anomalies from 1900–2005 is 0.006.

Location	r^2 values data trend	r^2 values residuals trend	Stdev data	Range	Regression coefficient
Scripps Pier, California	0.14	**0.19**	0.68	3.81	0.009
Pacific Grove, California	0.19	**0.22**	0.59	3.26	0.010
CCS - (34°N 118°W)	0.09	**0.13**	0.77	4.08	0.007
CCS - (32.5°N 122.5°W)	0.14	**0.21**	0.51	2.48	0.007
Gulf of Alaska (34°N 118°W)	0.16	**0.20**	0.47	1.97	0.006
Central Tropical Pacific (34°N 118°W)	0.20	**0.24**	0.47	2.04	0.007
Central North Pacific (36°N 170°W)	0.05	**0.12**	0.64	2.69	0.005
North Indian (8°N 90°E)	0.68	**0.72**	0.29	1.42	0.008

TABLE 2

Coefficients of determination (r^2 values) for the shared variability between the time series shown in Figure 3A–J. California Current System (CCS) COADS-based time series are the CCS–ERSST centered at 34°N and 118°W and the CCS–Kaplan SST series for the 5° x 5° grid centered at 32.5°N and 122.5°W (see figs. 1 and 2 for locations).

	PDO	Scripps Pier	Pacific Grove	CCS–ERSST	CCS–Kaplan SST	Gulf of Alaska	Central Trop. Pac.	Central North Pacific	North Indian
PDO	1.00								
Scripps Pier	0.44	1.00							
Pacific Grove	0.29	0.39	1.00						
CCS–ERSST	0.35	0.63	0.66	1.00					
CCS–Kaplan SST	0.36	0.64	0.63	0.83	1.00				
Gulf of Alaska	0.21	0.29	0.30	0.54	0.40	1.00			
Central Tropical Pacific	0.18	0.31	0.27	0.46	0.50	0.28	1.00		
Central North Pacific	0.48	0.27	0.16	0.13	0.18	0.04	0.09	1.00	
North Indian	0.07	0.21	0.24	0.24	0.17	0.25	0.34	0.00	1.00
Global average	0.03	0.26	0.32	0.37	0.24	0.40	0.32	0.03	0.74

Both the Kaplan SST and the ERSST data processing includes quality control (to eliminate outliers), data correction (to correct for methodology changes from buckets and ship intakes), and smoothing based on neighboring grids (Kaplan et al. 1998; Smith and Reynolds 2004). Prior to 1950, sampling error may result in a damping of variability and a tendency towards zero anomaly. Sampling error is greatest prior to 1880 and during years of World War (Smith and Reynolds 2004).

Although the selected time series are of insufficient length to confidently determine linkages between multiple decadal-scale patterns of variability with one another, the coefficients of determination (r^2 values) are calculated to show the amount of variability that time series share with one another and with the PDO over the length of the records. After regressing each SST series with the PDO, the residuals of the SST time series are examined to show the variability in the SST series that is not associated with the PDO. Causality of SST variability is generally discussed with respect to known processes rather than significance levels because low frequency variability produces a large degree of autocorrelation, which lowers significance of statistical measures.

To examine spatial characteristics of variability across different regions of the CCS, 10 m temperature variations at CalCOFI stations were examined. Annual mean temperature anomalies from 1950–2000 were calculated by averaging monthly anomalies from the long-term monthly mean. Annual average anomalies were calculated only if a station had been sampled three or more times during a given year. Since Santa Barbara Basin and Scripps Pier variations are of particular interest, we examined relationships from select CalCOFI stations along lines 80 and 93 as well as station 82 47 (over the Santa Barbara Basin). We also calculated an annual average of all CalCOFI stations near the Santa Barbara Basin (77 51, 77 55, 80 55, 82 47, 83 42, and 83 55) and call it the "CalCOFI Santa Barbara Basin region" (see fig. 2). Figure 2 additionally shows the area from which stations in the southern California Bight were averaged to form the "CalCOFI So. Cal. Bight region" (Sts. 87 35, 87 45, 90 30, 90 37, 90 45, 93 30, 93 35, 93 40) and the stations from the area offshore that were averaged to form the "CalCOFI offshore region" (Sts. 77 70, 77 80, 80 70, 80 80, 80 90, 83 70, 87 70, 87 80, 90 70, 90 80, 90 90, 93 70, 93 80, 93 90). CalCOFI stations farther

offshore of station 90 do not have sufficient observations in the early part of the record to calculate monthly averages for anomalies. The CalCOFI records were also compared with ERSST series from different regions of the CCS after 1950.

We compare and contrast the spatial patterns of SST anomalies during selected multi-year epochs from the 20th century. SST anomalies from the ERSST at the NOAA Climate Diagnostic Center (based on their 1971–2000 climatology) were averaged based on periods having similar and persistent patterns of foraminifera abundances from Santa Barbara Basin sediments that are described in detail by Field (2004a) and Field et al. (2006). However, the selection of intervals also matches multi-annual to decadal periods of the PDO and SST anomalies off California.

RESULTS

Temporal SST Variability

The time series of SST from the California Current System (CCS) and the PDO are shown in Figure 3 (A–E). The trend of increasing SST with time is quantified by linear regression and significant for all regions of the CCS (tab. 1). There is also considerable inter-annual- to decadal-scale variability in these records; a significant portion (29–44%) of this variability can be accounted for by the PDO (tab. 2).

Additional variability within the CCS can be attributed to regional- and global-scale variability not associated with the PDO. Explained variance (r^2 values; also referred to as levels of shared variability) in Table 2 show that the selected SST series from the CCS generally share more variability with one another than with the PDO. Figure 3 (K-N) shows the time series of the residuals of the SST series from their relationship with the PDO. There is greater shared variability between both the original CCS SST time series and the CCS residuals with the global average SST anomalies (tabs. 2 and 3) than can be explained by a linear trend with time (tabs. 1 and 2). Although the CCS makes up a part of the global SST data, it is thus apparent that CCS temperature variations are part of global temperature variations that are not best described by a linear trend.

The relationships between the PDO and the SST time series off California are shown before and after 1950 to examine systematic differences between time periods (fig. 4A, 4C, 4E, 4G). Because the PDO is a detrended measure, there is a notable offset in the relationship between the PDO and each SST time series. The shared variability between these variables within each shorter time period is stronger than the correlation between variables of the whole record (fig. 4). The offset in the relationship between time periods indicates that relationships between other variables (e.g., biological records) with either SST or the PDO will differ in long time series as well.

On the other hand, although the relationships between the SST time series from the CCS show some differences in slope, there is no apparent systematic offset (figs. 4B, D, F, H). The changes in the slopes of Pacific Grove and Scripps with COADS-based time series are opposite one another. The Scripps and Pacific Grove time series vary as much with each other as each of these series varies with the COADS series, except that Scripps Pier does not show highly negative SST anomalies in the early 20th century that are present in other time series. The levels of shared variability are not consistently higher or lower before and after 1950 (fig. 4). The tighter coupling between these SST records indicates that single regional temperature records reflect temperature variability within the CCS much better than the PDO over the 20th century.

ERSST series from other regions of the North Pacific and the Indian Ocean are shown in Figure 3 (F-I). The variability that they share with the PDO, with other SST series, and with time are shown in Tables 1 and 2. The residuals of those relationships are shown in Figure 3 (O-R) and the shared variability (r^2 values) between them and the residuals of the CCS series are shown in Table 3. Linear trends of averaged data are significant for all areas except in the central North Pacific, but there is a significant linear trend in the residuals of the central North Pacific. Some of the residual SST series from the CCS share considerable variance with other residual series from different regions of the North Pacific (with the exception of the central North Pacific), indicating that the PDO does not capture all of the shared basin-scale variability.

The linear trend in global mean SST over the 1900–2005 period is approximately 0.6 +/− 0.2°C (Smith and Reynolds 2004) while the range of interannual-interdecadal fluctuations, of which a portion is associated with the PDO, is 1.42–4.08°C (fig. 3 and tab. 1). The CCS time series contain warming trends ranging from +0.007°C/yr to +0.010°C/yr, which is similar to, but slightly higher than the +0.006°C/yr trend in global SST over 1900–2005 (tab. 1). It is noteworthy that warming trends at Scripps Pier and Pacific Grove are quite similar to those constructed in the CCS from the ERSST and Kaplan data sets, suggesting that the longer SST record estimated from the gridded SST data sets have been successfully corrected for changes in procedures (see also Rayner et al. 2005). The central North Pacific, which had a cooling trend from 1950–2000 (fig. 3), has had a warming trend of similar magnitude as the other regions, +0.005°C/yr, over this longer period. The North Indian Ocean also shows a similar trend as other

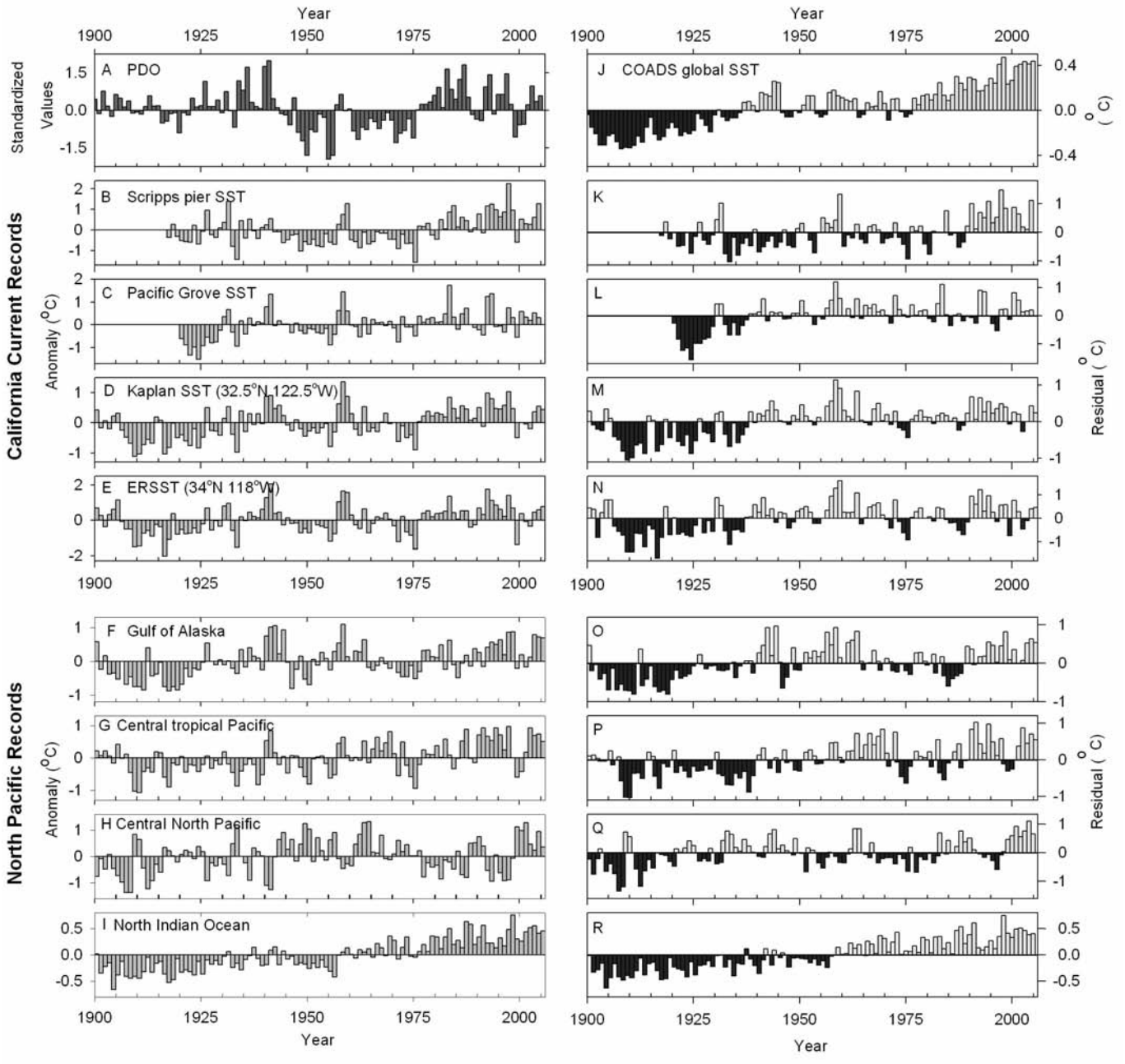

Figure 3. Time series of Sea Surface Temperature (SST) variability from A) the PDO index and different records from the California Current, B) Scripps Pier, C) Pacific Grove, D) Kaplan SST for the 5° × 5° grid centered at 32.5°N and 122.5°W, and E) ERSST for the 2° × 2° grid centered at 34°N and 118°W (fig. 2). Other ERSST records from the North Pacific are F) Gulf of Alaska, G) central tropical Pacific, H) central North Pacific, and I) the Indian Ocean (see fig. 1 for locations). J) The global average SST anomaly and K-R) the residuals of the relationship of each time series with the PDO are shown in the corresponding panels to the right.

regions (+0.008°C/yr), although the trend explains a large portion of the variability because interannual and decadal variability is reduced (tab. 1 and fig. 3).

Spatial Variability Within the California Current

Annual averages of temperature anomalies at 10 m for individual CalCOFI stations are compared with other records to examine spatial coherence in near-surface temperature variability within the CCS from 1950–2000 (fig. 5). The levels of shared interannual variability (r^2 values) are shown for individual CalCOFI stations with one another, with the more continuous coastal SST series (Scripps Pier and Pacific Grove), with the averages of multiple CalCOFI stations, and with the ERSST series (fig. 6; tab. 4). Figures 6A, 6C, and 6E show the levels of shared variability between three different individual

TABLE 3
Coefficients of determination (r^2 values) for the shared variability between the residual time series of Figure 3L–R and the global average in Figure 3J.

	Scripps Pier	Pacific Grove	CCS–ERSST	CCS–Kaplan SST	Gulf of Alaska	Central Trop. Pac.	Central North Pacific	North Indian
Scripps Pier	1.00							
Pacific Grove	0.18	1.00						
CCS–ERSST	0.39	0.52	1.00					
CCS–Kaplan SST	0.41	0.48	0.75	1.00				
Gulf of Alaska	0.08	0.13	0.41	0.25	1.00			
Central Tropical Pacific	0.14	0.14	0.35	0.39	0.17	1.00		
Central North Pacific	0.00	0.00	0.01	0.00	0.04	0.00	1.00	
North Indian	0.10	0.16	0.19	0.11	0.20	0.28	0.12	1.00
Global average	0.18	0.26	0.39	0.24	0.39	0.31	0.16	0.72

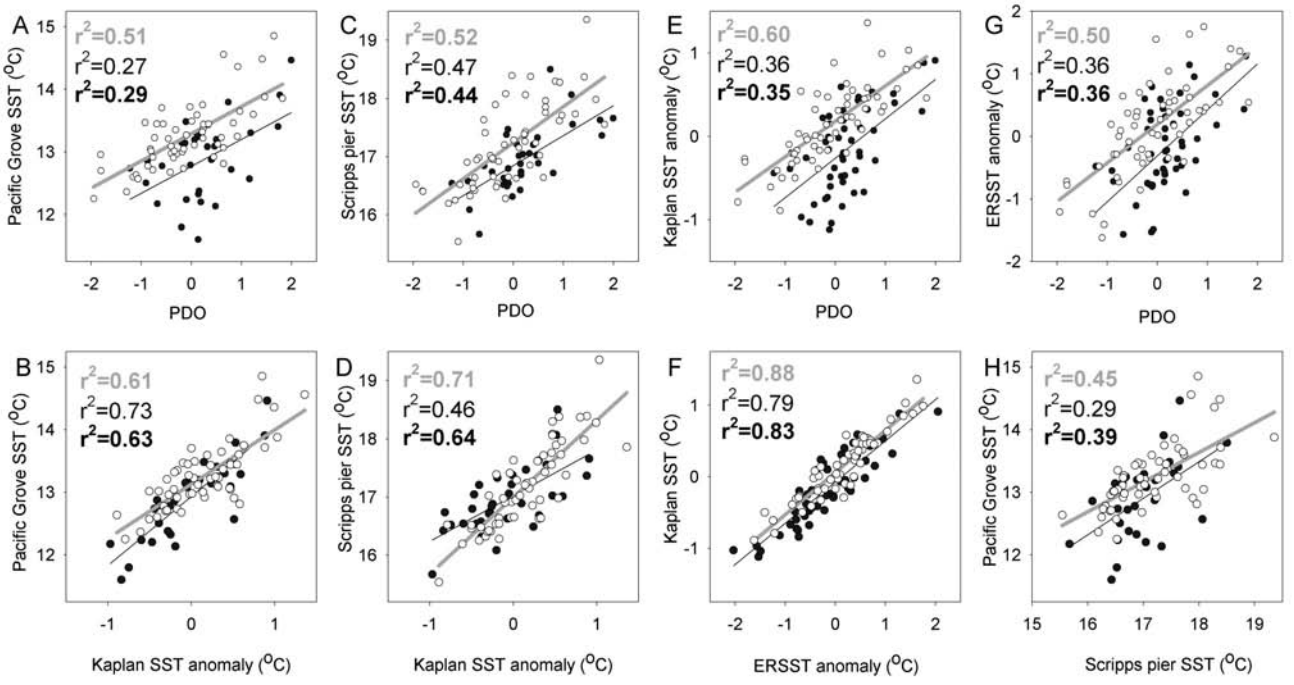

Figure 4. Relationships between SST series from the California Current System with the PDO (A, C, E, G) and with other SST series off of California (B, D, F, H). Dark circles and dark thin line are the relationship between 1900–50 and light circles and thick grey line are 1951–2005. Coefficients of determination (r^2 values) are shown for the period from 1951–2005 (top/gray), 1900–50 (middle/dark), and 1900–2005 (bottom/bold).

CalCOFI stations with other stations that represent the main patterns in Table 4. CalCOFI stations that are close to each other generally have the highest levels of shared variability. However, the levels of shared variability often weaken for stations along cross-shore gradients, particularly along line 80. For example, the station over the Santa Barbara Basin (82 47) has strong shared variability with nearby stations and within the coastal domain but weaker levels of shared variability with stations 80 70 and 80 90.

Comparing Figures 6A, 6C, and 6E with Figures 6B, 6D, and 6F shows the degree to which annual averages of multiple CalCOFI station anomalies have higher levels of shared variability with other time series than do annual averages from an individual CalCOFI station (see also tab. 4). The number of measurements composing the individual CalCOFI station annual averages (three to twelve measurements per year with a mode of four) is as many as one or two orders of magnitude less than the continuous time series or the spatial averaged SST series. Figure 7 illustrates that there are still some reductions in levels of shared variance between the more continuous ERSST series and Scripps Pier series with other records as distance-between-records increases (tab. 5), but no clear cross-shore differences.

Ecosystem Variability from Fossil Foraminifera

Because SST variations around the Santa Barbara Basin location are representative of those on a larger scale, we can use abundances of fossil foraminifera from Santa

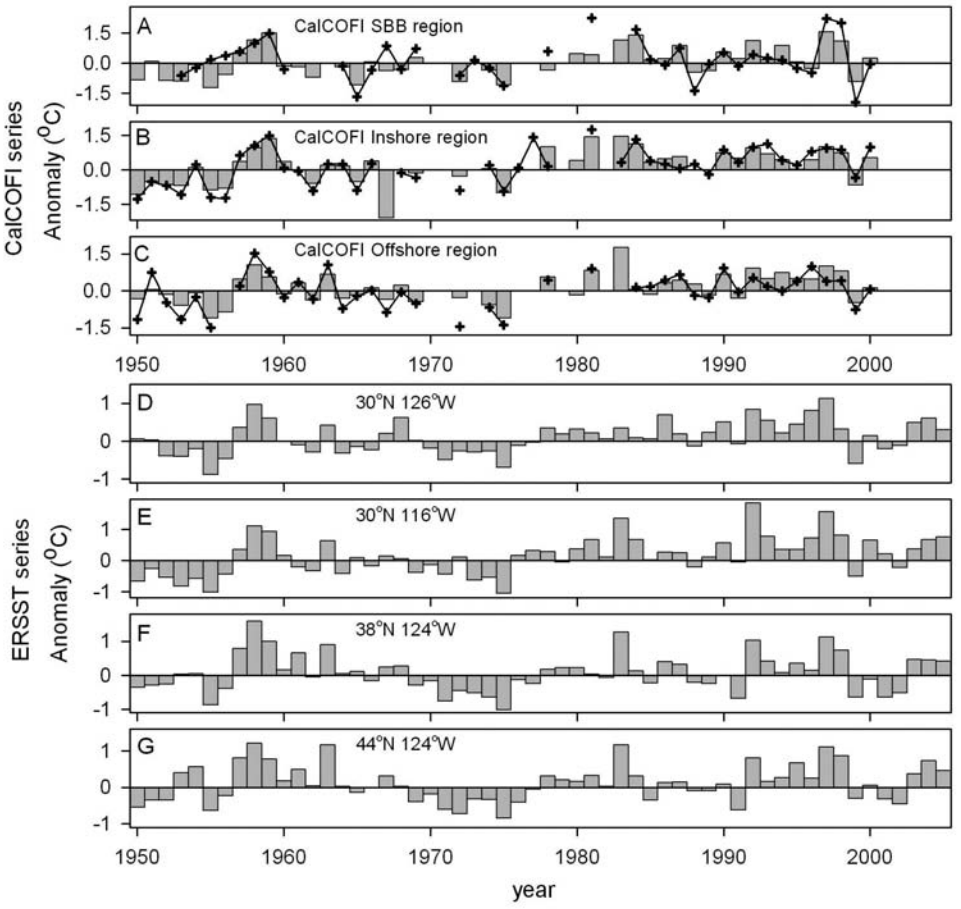

Figure 5. Time series of 10m temperature variability from A) the CalCOFI Santa Barbara Basin region (vertical bars) and CalCOFI station 82 47 (+), B) the CalCOFI Inshore region (vertical bars) and CalCOFI station 93 30 (+), C) the CalCOFI Offshore region (vertical bars) and CalCOFI station 93 90 (+). Also shown are ERSST series for the 2° × 2° grids at D) 30°N 126°W (offshore Southern California), E) 30°N 116°W (Baja California), F) 38°N 124°W (central California), and G) 44°N 124°W (Oregon; see fig. 2 for locations).

TABLE 4

Coefficients of determination (r^2 values) for the shared variability between the annual averages of individual CalCOFI stations with one another and with other time series from the California Current from 1950–2000 (see fig. 2). CalCOFI SBB region refers to the annual average of stations around the Santa Barbara Basin. Dashes denote time series that share data and thus should not be considered.

	St. 82 47	St. 80 55	St. 80 70	St. 80 90	St. 93 30	St. 93 50	St. 93 70	St. 93 90
St. 82 47	1.00							
St. 80 55	0.65	1.00						
St. 80 70	0.42	0.60	1.00					
St. 80 90	0.18	0.43	0.54	1.00				
St. 93 30	0.40	0.55	0.56	0.45	1.00			
St. 93 50	0.51	0.60	0.54	0.41	0.53	1.00		
St. 93 70	0.31	0.52	0.64	0.41	0.48	0.66	1.00	
St. 93 90	0.29	0.43	0.42	0.43	0.61	0.60	0.56	1.00
CalCOFI SBB region	—	—	0.56	0.36	0.70	0.63	0.41	0.45
CalCOFI So. Cal. Bight	0.59	0.66	0.56	0.40	—	0.72	0.53	0.69
34°N 118°W (So. Cal. Bight)	0.53	0.64	0.61	0.41	—	0.57	0.62	0.52
Scripps Pier	0.52	0.61	0.64	0.55	0.68	0.54	0.69	0.48
CalCOFI offshore	0.37	0.59	—	—	0.65	0.65	—	—
30°N 126°W (offshore)	0.41	0.53	0.58	0.56	0.58	0.48	0.57	0.66
30°N 116°W (baja)	0.44	0.60	0.64	0.56	0.63	0.55	0.67	0.47
Pacific Grove	0.30	0.37	0.35	0.24	0.36	0.32	0.42	0.21
38°N 124°W (northern Cal.)	0.47	0.54	0.67	0.43	0.45	0.56	0.62	0.59
44°N 124°W (Oregon)	0.38	0.49	0.67	0.50	0.42	0.53	0.67	0.59

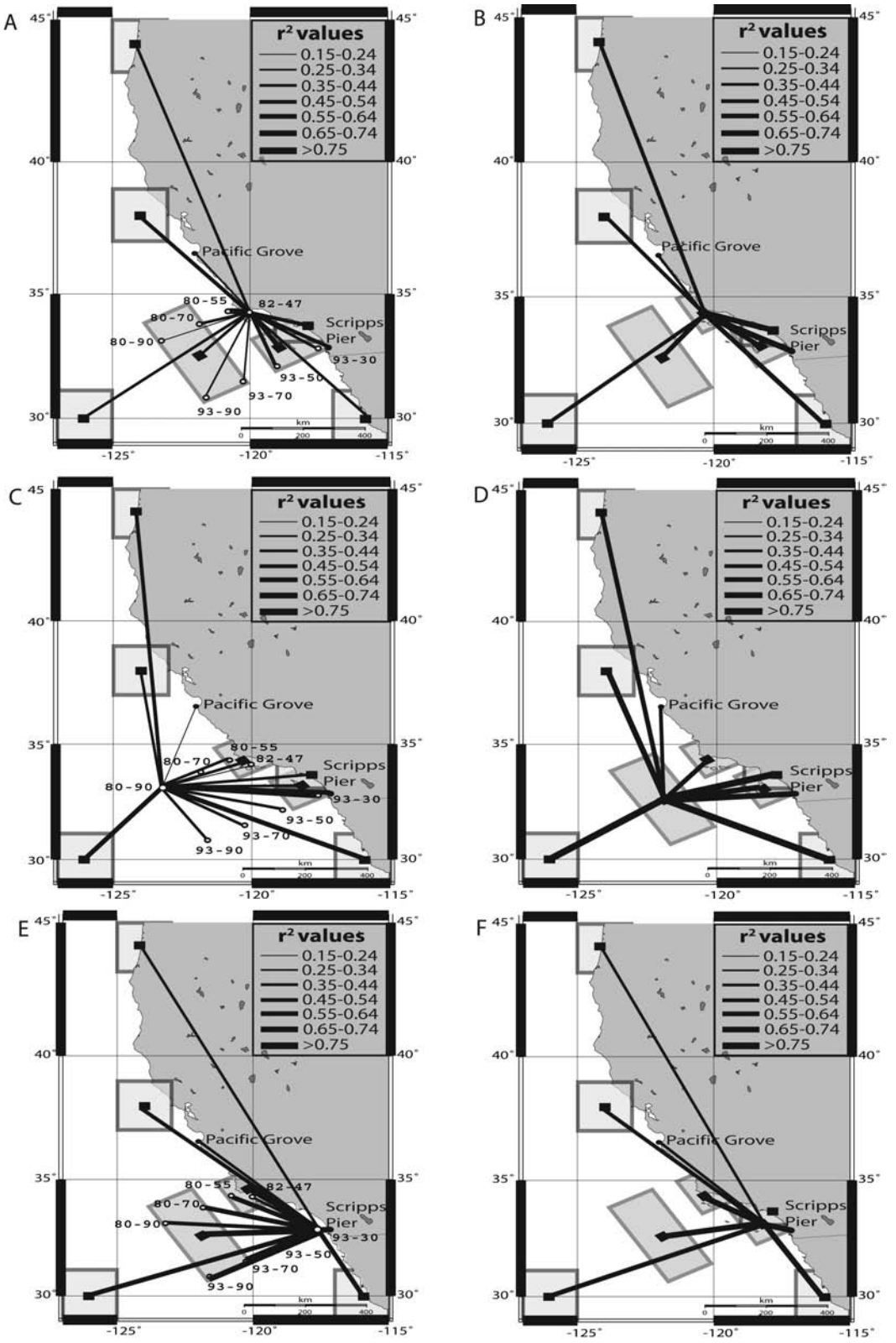

Figure 6. Maps of the California Current showing levels of shared variability (r^2 values) between individual CalCOFI annual averages at A) Station 82 47, C) Station 80 90, and E) Station 90 30 with other individual CalCOFI stations, with ERSST series, continuous coastal SST series (Scripps Pier and Pacific Grove), and annual averages of multiple CalCOFI stations within a given region. Also shown are levels of shared variability between the annual averages of multiple CalCOFI stations located near or within, B) the Santa Barbara Basin area (82 47), D) the offshore region (80 90), and F) the Southern California Bight region (90 30).

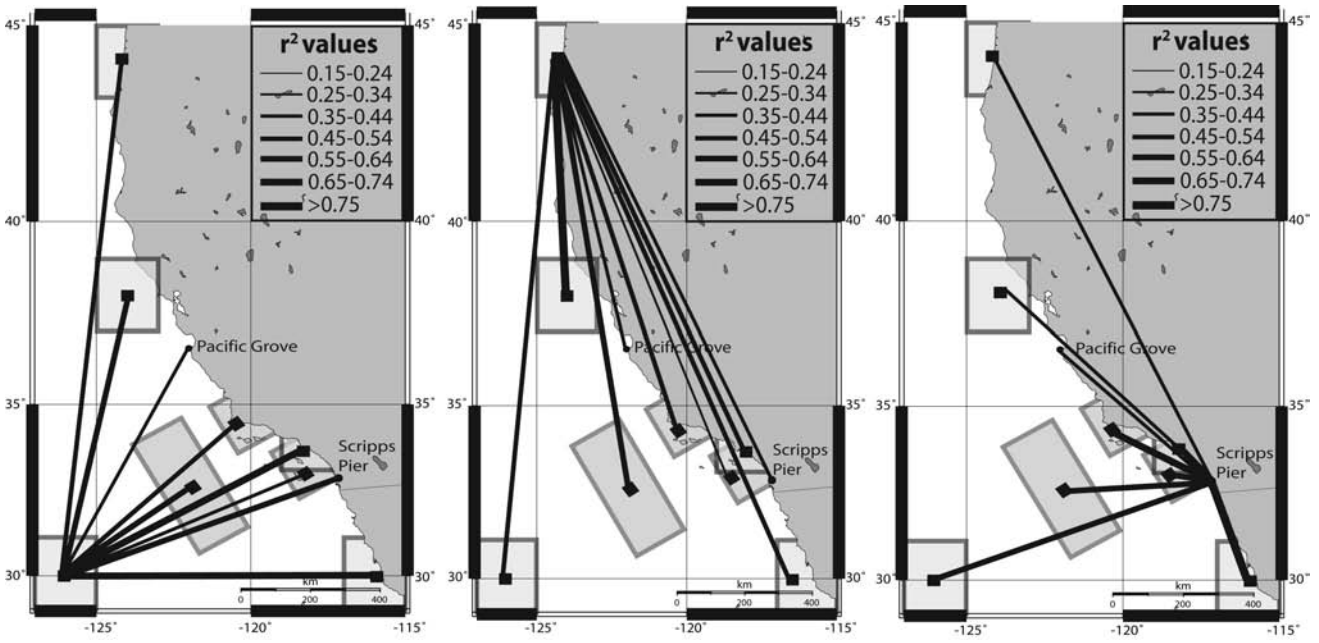

Figure 7. Levels of shared variability (r^2 values) between three different SST series with other regions in the California Current System (as in fig. 6). A) The 2° × 2° grid ERSST series located at 30°N 126°W, B) the 2° × 2° grid ERSST series located at 30°N 126°W, and C) Scripps Pier.

TABLE 5

Coefficients of determination (r^2 values) for the shared variability between annual averages of CalCOFI stations within a given region and with other time series from the California Current from 1950–2005 (fig. 2). Dashes denote time series that share data and thus should not be considered. ERSST series are indicated by the location of the center of the 2° × 2° grid (and region of the coastline).

	CalCOFI SBB	CalCOFI So.Cal.Bight	34N 118W	Scripps Pier	CalCOFI offshore	30N 126W	30N 116W	Pacific Grove	38N 124W	44N 124
CalCOFI SBB region	1.00									
CalCOFI So. Cal. Bight	0.62	1.00								
34°N 118°W (So. Cal. Bight)	0.67	—	1.00							
Scripps Pier	0.67	0.62	0.66	1.00						
CalCOFI offshore	0.55	0.59	0.73	0.62	1.00					
30°N 126°W (offshore)	0.50	0.42	0.73	0.63	0.63	1.00				
30°N 116°W (baja)	0.63	0.59	0.82	0.75	0.73	0.72	1.00			
Pacific Grove	0.44	0.40	0.63	0.44	0.56	0.43	0.62	1.00		
38°N 124°W (northern Cal.)	0.49	0.42	0.68	0.39	0.68	0.61	0.61	0.55	1.00	
44°N 124°W (Oregon)	0.46	0.41	0.54	0.39	0.63	0.48	0.53	0.38	0.86	1.00

Barbara Basin sediments to extend the 1900–2005 instrumental record of ocean climate further back in time (Field 2004a; Field et al. 2006). Figure 8A shows the temporal variations in the first two principal components (PC) of the abundances of nine groupings of species (Field et al. 2006). Also shown are the abundances of three individual species and the sum of five different "rare subtropical species" that exemplify the patterns summarized by the principal components. Rare subtropical species and the primarily subtropical species, *Orbulina universa*, have strong loadings on PC-1. Subpolar *Neogloboquadrina pachyderma* (sin.) has a negative loading on PC-1 and a positive loading on PC-2. Temperate *Turborotalita quinqueloba* has a positive loading on PC-2 (Field et al. 2006).

PC-1 characterizes a 20th-century trend of increasing abundances of tropical and subtropical species as well as a decrease in abundance of the subpolar *N. pachyderma* (sin.). After 1925, the tropical and subtropical species sustain higher abundances than prior centuries, although with considerable multi-annual to decadal variability throughout the record. An increase in *O. universa* after the mid-1970s reflects increasing favorable conditions for species associated with PC-1.

PC-2 characterizes an assemblage of temperate and subpolar species that generally live within the thermocline and are primarily affected by variations in subsurface temperatures rather than SST (Field 2004b). The initial increase in PC-1 around 1925 was associated with favorable conditions for *T. quinqueloba* but the stronger

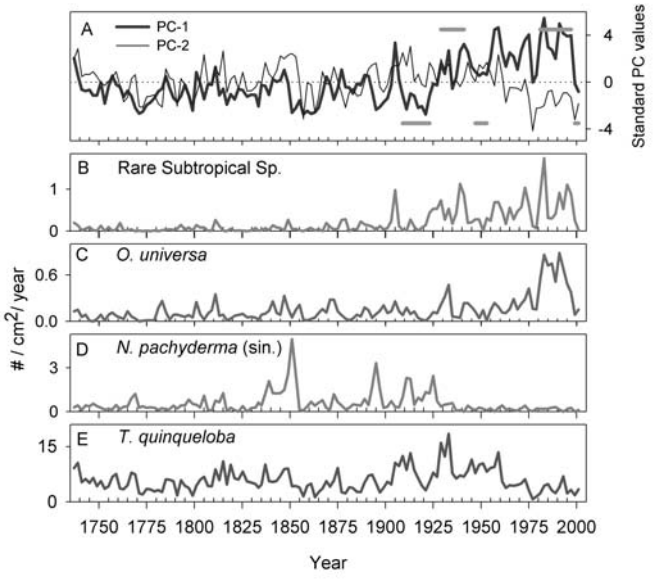

Figure 8. A) Temporal variations of a principal component (PC) analysis of the annual fluxes of planktonic foraminifera from two-year sampling intervals of Santa Barbara Basin sediments (from Field et al. 2006) and the temporal variations of several species that reflect the main variations of the PCs. Species that are of tropical and subtropical origin and show trends of increasing abundances are B) The combined abundances of *G. calida*, *G. rubescens*, *G. glutinata*, *G. siphonifera*, and *G. digitata*, and C) *O. universa*. Species that are of temperate and subpolar geographic affinities and show no trend are D) *N. pachyderma* (sin.), and E) *T. quinqueloba*. Horizontal bars in Figure 8A indicate selected time periods to illustrate spatial patterns of SST anomalies (fig. 9) based on foraminiferal variations and the PDO index (see text).

warming in the late 20th century results in increasingly unfavorable conditions for all species associated with PC-2. Although the low values of PC-2 after the mid-1970s are not unique to this series, the divergence of PC-1 from PC-2, which began around 1960, marks a distinct change in the relationship pf PC-1 and PC-2.

The foraminiferal variations summarized by PC-1 are compared with the different long-term SST time series off of southern and central California averaged into two-year intervals that correspond with the sedimentary chronology. PC-1 shows the strongest correlations with the Kaplan SST index ($r^2 = 0.32$; $p < 0.005$) but also significant relationships with the Pacific Grove series and ERSST at 34°N and 118°W ($r^2 = 0.23$; $p < 0.005$ and $r^2 = 0.29$; $p < 0.005$ respectively). However, there is very little shared variability between PC-1 with Scripps Pier SST ($r^2 = 0.09$) or the PDO index ($r^2 = 0.01$), primarily since PC-1 is strongly negative in the early 20th century and the anomalies of Scripps Pier SST and the PDO are not. Although shared variability is lower than variability shared between SST series off California (tab. 2), the two-year sampling intervals have some error associated with them (Field 2004a).

Spatial Patterns of North Pacific SST Variability

It is of interest to determine if regional variations of SST and the effect SST has on marine populations in the CCS are associated with basin-scale patterns. We use the foraminiferal record to select decadal-scale time periods of ocean climate that correspond with similar phases of the PDO. Upper (lower) horizontal bars in Figure 8A correspond with periods of relatively greater (lesser) abundance of tropical and subtropical species and positive (negative) PDO values. Periods selected include relatively cool episodes in 1909–24, 1947–54, and 1999–2001 and relatively warm episodes in 1929–42, 1981–98, and 2003–05.

The period from 1909–24 has predominantly negative anomalies in the CCS, despite only slightly negative to neutral values of the PDO (fig 3). Figure 9A indicates that SST anomalies are strongly negative throughout the eastern North Pacific and much of the tropical Pacific, while only the central North Pacific and Kuroshio extension are near the 1971–2000 average. This time period also corresponds with the lowest global SST anomalies of the record (fig. 3J). However, the foraminiferal indices (fig. 8) indicate that the CCS was frequently this cool over the last several centuries.

The period from 1929–42 marks the first pulse of 20th century warming (fig. 3B-E, fig. 3J; Enfield and Mestas-Nuñez 1999), which is particularly evident in the long-term foraminiferal record (fig. 8A). Although this time period corresponds with a positive phase of the PDO, the positive SST anomalies are primarily centered in the Gulf of Alaska. Contrary to recent, well-known teleconnections, this period shows negative SST anomalies in the tropical Pacific. PC-2 indicates negative subsurface temperature anomalies in the CCS at this time.

In 1947–54, there were negative SST anomalies in the CCS and a spatial dipole of SST anomalies typical of a negative phase of the PDO (fig. 9B). Even though PC-2 indicates subsurface conditions favorable for temperate and subpolar species from 1947–54, conditions during previous centuries were frequently more favorable for the subpolar species *N. pachyderma* (sin.) and usually less favorable for tropical and subtropical species.

While the PDO index suggests that the warm period from 1981–98 is similar to other decadal periods of elevated PDO (fig 3A), the PCs of foraminiferal abundances indicate an atypically warm water column in the CCS following the mid-1970s warming (fig 8). Comparison of Figure 9E with Figure 9D reveals several noteworthy differences between the spatial pattern of SST anomalies during these two decadal time periods (1929–42 and 1981–98). First, there is an extension of positive SST anomalies through the southern region of the CCS to the tropics from 1981–98. Second, there are large negative anomalies in the western Pacific and Indian Ocean during the 1929–42 time period, but not during the late 20th century.

The most recent cool period from 1999–2001 has a spatial pattern of anomalies similar to a typical negative

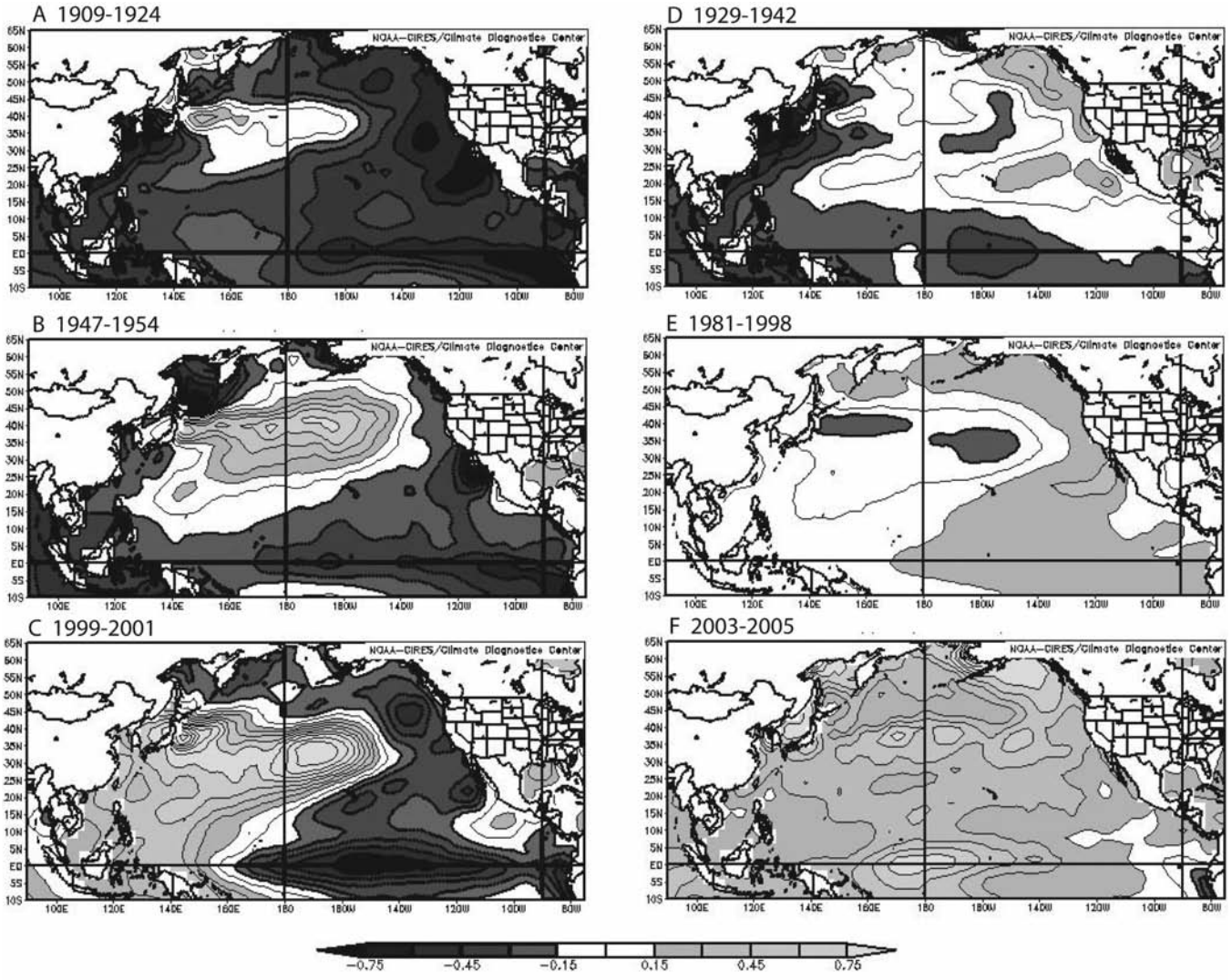

Figure 9. Spatial patterns of SST anomalies throughout the North Pacific during time periods that correspond with particular patterns of foraminiferal variations and SST variability (see text and fig. 8A). Anomalies are based on the time period from 1971–2000. Panels on the left (right) correspond with negative (positive) phases of the PDO.

PDO phase, despite being based on only three years (fig. 9E). However, the PCs indicate that the California Current was only slightly cooler from 1999–2001 than the long-term average of the last several centuries. Note the strongly positive SST anomalies in the western and central North Pacific relative to other negative PDO phases.

Recently, the PDO index has been positive from 2003–05, although the foraminiferal record does not extend beyond 2001. However, the distribution of positive SST anomalies from 2003–05 is more extensive than during other positive PDO phases (fig. 9F) and there are no regions of notable negative anomalies. In summary, Figure 9 illustrates how the magnitude and spatial extent of positive SST anomalies increase in time during different phases of the PDO.

DISCUSSION

The Warming Trend

The discussion is centered on aspects of the warming trend, spatial variability in SST and the processes that produce it, and the resulting effects on marine populations, particularly within the CCS. While a large portion of the variability throughout the North Pacific can be explained by processes associated with the PDO, a long-term secular trend is nearly as important (tabs. 1 and 2). Regional and global processes account for additional variability in the records examined. The PDO only partially captures the variability of SSTs in the North Pacific during the 20th century because the PDO has been constructed from a filtered data set in which the global trend in SST was removed. Thus the gridded SST-

derived time series should be more accurate indicators of regional SSTs than the PDO, despite times of poor data coverage and instrumental and measurement changes.

Before considering causes of SST variability, it is important to note that the time series considered here are short relative to the decadal and longer timescales. There may be artificial relationships with the PDO and especially the trends due to autocorrelation when there is no causality for the relationships. For example, although Figure 1 indicates that the Indian Ocean and western Pacific share substantial variability with the PDO from 1948–2005, the longer record from the Indian Ocean (fig. 3I) has less shared variability with the PDO but is more similar to the global average SST anomaly (tab. 2). Thus it is possible that, due to the short records that are available, spurious correlations can occur between time series with the PDO since the PDO has a trend after 1950 ($r^2 = 0.30$) but not over the length of the record since 1900.

Processes acting on global scales may be important for SST variability in the North Pacific since the SST series shown in Figure 3 share nearly as much variance with the global average SST as they share with the PDO (tab. 2). Although much of this variability can be explained by a linear regression, the near zero anomalies at the onset of the 20th century suggest a mode of variability in global SSTs that is not just a linear trend (Enfield and Mestas-Nuñez, 1999).

Aggregated SST records from the Atlantic, Indian, and Pacific Ocean basins appear to contain evidence for solar forcing over very coherent global scales (White et al. 1997; White et al. 1998), a connection that seems to hold up until about 1970, when greenhouse gas forcing becomes a larger influence (White et al. 1998; Cubash and Meehl 2001). Early 20th-century warming may also reflect the final ending stage of the Little Ice Age (Esper et al. 2002) and reduced volcanic forcing (Crowley 2000). Additionally, models indicate that greenhouse gas accumulation may have been sufficient to affect oceanic heat content since about 1930 in regions where stratification could limit mixing and concentrate heat gain to the near surface (Barnett et al. 2001), such as the California Current. Regardless of cause, early 20th-century warming matches the highest observed levels of natural variations in tropical and subtropical species within the CCS (fig. 8A) as well as northern hemisphere air temperatures (Mann et al. 1999).

The linear trends in North Pacific and global SST anomalies (fig. 3J-R) are consistent with a documented upward trend in heat content of the global oceans from the surface to 3000 m (Levitus et al. 2000; 2001). The global heat content averages across regional variations arising from horizontal and vertical redistribution of heat within the oceans and reveals that the oceans have gained a substantial amount of heat since 1955 that can only be of atmospheric origin (Levitus et al. 2000; 2001; Barnett et al. 2005). Accumulating greenhouse gasses in the atmosphere is the only adequate explanation available for (a) the amount of heat absorbed by the ocean and (b) the observation that the increase in temperatures is greatest in the near-surface (White et al. 1998; Levitus et al. 2001; Barnett et al. 2005).

While some of the near-surface warming in the 20th century is attributed to anthropogenic activity, the relative contributions of greenhouse gases to the timing and magnitude of 20th-century warming remain unclear. Nonetheless, it is important to consider that records beginning after about 1925 lie within an unusually warm period and may not capture the full range of variability that has occurred over the last few centuries.

California Current Variability

Examination of the SST residuals from the PDO (fig. 3K-R) reveals that the warming trend is not uniform throughout the North Pacific. Using an ocean model forced by meteorological input, Di Lorenzo et al. (2005) showed that warming in the CCS can only be adequately explained by ocean-atmosphere heat flux over a large area of the eastern North Pacific and the advection of this water into the California Current region. Thus, warming patterns primarily result from the coupling of variations in horizontal advection and other processes with large-scale changes in ocean-atmosphere heat flux, rather than local-to-regional heat fluxes (Di Lorenzo et al. 2005).

Near-surface temperature variations in the CCS are similar across regions, including over the Santa Barbara Basin (McGowan et al. 1998; tabs. 3 and 4). Existing regional and thermocline differences are secondary to the dominant patterns of warming and cooling (Mendelssohn et al. 2003) and are greatly reduced when a sufficient number of measurements are averaged (fig. 6 and tab. 4).

The Scripps Pier SST time series is perhaps the most well-known of all SST series in the CCS and shows some of the highest levels of shared variability with other regions of the CCS since 1950 and with the PDO. However, the Pacific Grove series, COADS-based series, and PC-1 all indicate that the early 20th century was one of the coolest periods in the CCS on record, whereas the Scripps Pier series shows moderately negative SST anomalies. These patterns of variability are consistent with a greater influence of upwelling and the flow of the California Current from 1909–24 (figs. 3 and 9) that were less influential at Scripps Pier within the Southern California Bight.

The North Pacific Index (NPI) shown in Figure 10 reflects the cyclonic activity of the Aleutian low (Trenberth and Hurrell 1994) and indicates that basin-

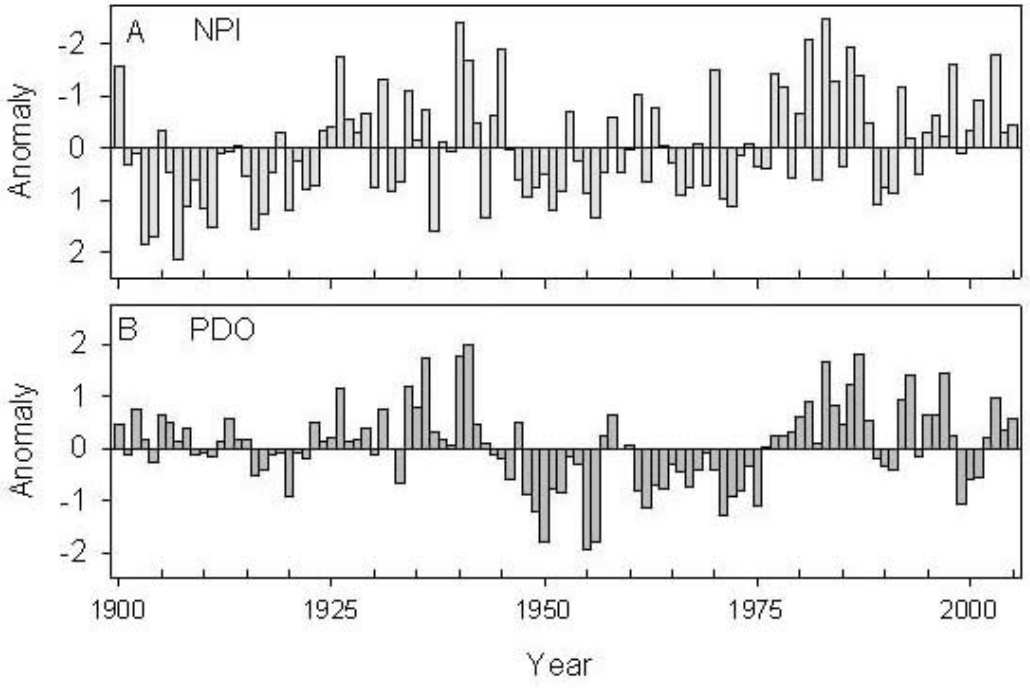

Figure 10. Indices of North Pacific climate variability from A) the NPI of cyclonic activity of the Aleutian low and B) the PDO. The NPI is the area-weighted sea level pressure over the region 30°N–65°N, 160°E–140°W from November to March (Trenberth and Hurrell 1994). There is a significant linear trend reflecting greater cyclonic activity of the Aleutian low (NPI, $r^2 = 0.10$, $p < 0.01$) but no trend in the PDO.

scale forcing can account for the patterns of variability from 1909–24. The NPI during this period is consistent with anomalously high pressure over the North Pacific that would intensify regional upwelling, flow of the California Current, and/or basin-scale Ekman pumping that shoals the water column in much of the eastern North Pacific (fig. 9A).

Processes of Change Related to the Trend

Although both the NPI and PDO are considered similar indicators of North Pacific climate, they have different patterns in the early part of the record (fig. 10). The NPI has a significant trend. The spatial SST patterns observed in Figure 9A are consistent with a reduction in the strength of the Aleutian low from 1909–1924, as inferred by the NPI, but not the PDO. The decadal differences between the NPI and the PDO reiterates that the detrended PDO may have different relationships with other environmental variables throughout the length of the instrumental records.

The trend in the NPI may be related, in part, to increasing SSTs in the tropical Pacific and Indian Ocean. Theoretical arguments, models, and observations over the last 100 years indicate that atmospheric pressure over the North Pacific is linked to convective activity in lower latitudes (Graham et al. 1994; Graham 1995; D'Arrigo et al. 2005; Schneider and Cornuelle 2005). Convective activity is greatest over regions of highest SSTs, and correlations of the NPI with tropical SSTs are strong in the western tropical Pacific, tropical Indian Ocean, and subtropical central Pacific (Graham 1995; Deser et al. 2004; D'Arrigo et al. 2005; Schneider and Cornuelle 2005). While correlations over these timescales are not sufficient to indicate a causal chain, there is a predominance of higher SSTs in these regions (e.g., figs. 3I and 9) in recent decades despite the negative anomalies in the central and eastern tropical Pacific from 1999–2001 (fig 7C).

The trend towards lower atmospheric pressure over the North Pacific could act in conjunction with variations in the position of the Aleutian low. Bond et al. (2003) noted that the spatial distribution of atmospheric pressure from 1999–2002 is partly similar to other negative PDO phases off California, but characterized by much lower pressure over the Gulf of Alaska and Bering Sea. Bond et al. also noted large differences in SST patterns between 1999–2002 and other periods. Figure 9 illustrates that different time periods throughout the 20th century generally have different patterns of SST variability despite similar signs of the PDO.

Another difference between the NPI and PDO is that the NPI has greater interannual variability than the PDO (fig. 10). Greater "memory" of the ocean relative to the atmosphere is one reason why the PDO may be a useful indicator of environmental conditions that affect marine populations. Additionally, the PDO also captures variability associated with the flow of the Kuroshio ex-

tension and other processes associated with ENSO, thus does not reflect the dynamics of any single process (Schneider and Cornuelle 2005).

Implications for Marine Ecosystems

The foraminiferal record is well-suited to show the effects of the warming trend on marine populations, since the composite of many species reflects SSTs and the record extends well beyond the 20th century. The optimum habitat of different species generally occurs with some amount of near-surface stratification—either in the form of a deeper thermocline or increased gradient across the thermocline, depending on the species (Field 2004b). Variations in SST and stratification likely affect species associated with PC-1 by stabilizing the water column to either concentrate prey in higher densities or decrease productivity and increase light levels, which is favorable for most tropical and subtropical species (that have symbiotic algae).

Just as different planktonic foraminifera species vary in response to interannual and decadal variations that depend on the life history and unique relationship with particular environmental variables (Field 2004b), so do other zooplankton and marine taxa (Rebstock 2001; Lavaniegos and Ohman 2003; Brinton and Townsend 2003). Nonetheless, it is worth discussing the implications of the historical reconstructions of planktonic foraminifera for other marine populations.

Instrumental or biological records that began by 1925 or thereafter may not reflect the ocean conditions and associated ecosystems that have been typical of the CCS over the last few centuries. Barry et al. (1995) showed that, like foraminifera, warm-water species of intertidal organisms at Pacific Grove increased in abundance between two different sampling intervals from 1931–33 and 1993–94. Semi-continuous CalCOFI hydrographic surveys and plankton collections, which began in 1950, show that the early 1950s was one of the coolest time periods with the highest zooplankton biomass in the CalCOFI time series (McGowan et al. 1998). Both the Barry et al. study and CalCOFI observations probably underestimate the impact of the current warming trend on marine populations because since 1925, the abundances of the "rare subtropical species" grouping of foraminifera has been higher than previous centuries. Studies characterizing ecosystem responses to temperature variations in the North Pacific during the early 20th century (e.g., Becker and Beissinger in press) should use regional SST records rather than the PDO in order to adequately capture the range of temperature variability that has been affecting marine ecosystems.

Many different trophic levels of pelagic communities have been affected by the warming since the mid-1970s (McGowan et al. 1998; Brinton and Townsend 2003; Lavaniegos and Ohman 2003). The foraminiferal changes in the late 20th century can be considered an indirect consequence of anthropogenic activity since they are linked to variations in SST which has increased, in part, due to greenhouse gasses (Field et al. 2006). As many of the other observed changes in marine ecosystems are linked to variations in SST and the associated effects of SST on water column that, in turn, affect productivity and pelagic habitats, many of these changes may be atypical of prior ecosystem variability.

However, different taxon respond to different physical mechanisms and/or have different sensitivities to variability in SST. Many changes associated with the 1977 ecosystem "regime shift" may be caused by other physical changes that are indirectly associated with, but not caused by, anomalous SSTs. Vertical mixing associated with wind-driven cyclonic activity, may be the largest decadal-scale influence in the central North Pacific (Venrick et al. 1987). In much of the Gulf of Alaska, stability of the water column and productivity are primarily affected by salinity, with changes in temperature acting as a less influential covariant (Gargett 1997). Variability in flow of the subarctic gyre into the Gulf of Alaska and the California Current may also be an important mechanism for marine populations (Chelton et al. 1982). Thus, some population changes may correspond strongly to variations in the PDO associated with mixing, freshwater input, and variations in flow rather than to variations in temperature (fig. 10). However, the possibility that the trend in atmospheric circulation is driven by changes in tropical SSTs may imply different mid-latitude forcing in the future.

The warming of the CCS in the 20th century coincides with anthropogenic influences on many mammals and fishes, which can have subsequent cascades to lower levels (Jackson et al. 2001). Many populations of seals, sea lions, and whales that feed on lower trophic levels were commercially extinct by the late 19th century (Field et al. 2001). The recovery of many of these marine mammal populations in the 20th century coincided with the intensification of many commercial fisheries (Field et al. 2001). Thus our understanding of the relationship between climate and marine populations is largely based on a time period of a modified ecosystem and unusually warm ocean temperatures.

A continued warming and exploitation of marine resources will most likely continue in the 21st century (Houghton et al. 2001) with different modes of variability than the 20th century. Extant marine lineages in the CCS have undergone many larger changes in climate than the ecosystem shift of the mid-1970s. Much larger shifts in temperature occurred within decades repeatedly throughout the last glaciation (Hendy and Kennett 1999). However, future ecosystem changes

will occur within a warmer ocean than they did during the last glacial period. The sensitivity of climate and ecosystem thresholds associated with future warming are entirely unknown. Understanding and anticipating future changes will require continued monitoring to obtain comprehensive regional observations and ongoing experiments with realistic global and regional models to differentiate specific mechanisms of variability from the warming trend that is affecting the ocean and its resources.

CONCLUSIONS

SST anomalies of annually-averaged data from individual stations and area averages in the California Current System have considerable variability at interannual to multidecadal time scales. The PDO accounts for approximately 29–44% of the variance in different records, which have a total range of 2–4°C since the early 20th century. On the other hand, a warming trend, estimated from linear regression, ranges from 0.6–1.0°C during the 20th century and accounts for nearly as much (26–37%) of the SST variability as the PDO. There are similar upward trends in other regions of the North Pacific (and Indian Ocean), although correlations with the PDO differ.

There are few differences in the patterns of near-surface temperature variability within the CCS since 1950, including around the Santa Barbara Basin. A record of abundances of planktonic foraminifera from Santa Barbara Basin sediments, along with COADS-based SST series and Pacific Grove SSTs, indicate that the early 20th century had strong negative SST anomalies persisting for multiple years to decades. These negative anomalies resulted from higher atmospheric pressure off of California that drove the flow of the California Current and upwelling prior to the onset of 20th-century warming. Although this variability is not reflected by the PDO or Scripps Pier record within the Southern California Bight, the foraminiferal record suggests that these negative anomalies are typical of regular variability during prior centuries, but that the strong warm anomalies in the latter 20th century are quite atypical.

Temperature and ecological records that began after 1930 may underestimate the range of ocean variability typical of prior centuries because they do not capture the negative extremes of variability. In particular, records that began after the mid-1970s lie within a period that has already become influenced by greenhouse gas-induced warming and would thus underestimate the influence of the warming trend and its effect on marine populations. Because the long-term trend is removed from the PDO, this index has a different relationship with associated variables during the early 20th century than in later periods. When considering changes spanning most of the 20th century, oceanic and ecosystem changes that are driven by atmospheric circulation may be better represented by the NPI than the PDO, while processes driven by changes in SST may be better represented by regional or larger scale measures of SST from COADS or similar SST data sets.

ACKNOWLEDGEMENTS

Development of the foraminiferal record was supported by University of California ship funds support to D. Field and University of California Coastal Initiatives grant 01T CEQI 06 1082 to Field and Charles. Shirley and Bill Kimmich were also gracious supporters of D. Field. Development of the foraminiferal records was also supported by NOAA Climate and Global Change grant NA36GP0479 and NSF Climate Dynamics grant ATM 94-06510 to T. R. Baumgartner as well as NSF OCE96-13596 and OCE01-10300, and California Current Ecosystem LTER support to M. D. Ohman. DRC was supported by the California Energy Commission PIER Program, the Department of Energy, and the California Department of Boating and Waterways.

LITERATURE CITED

Barnett, T. P., D. W. Pierce, K. M. AchutaRao, P. J. Gleckler, B. D. Santer, J. M. Gregory, and W. M. Washington. 2005. Penetration of human-induced warming into the world's oceans. Science 309:284–287.

Barnett, T. P., D. W. Pierce, and R. Schnur. 2001. Detection of Anthropogenic Climate Change in the World's Oceans. Science 292:270–274.

Barry, J. P., C. H. Baxter, R. D. Sagarin, and S. E. Gilman. 1995. Climate-related, long-term faunal changes in a California rocky intertidal community. Science 267:672–675.

Baumgartner, T. R., A. Soutar, and V. Ferreira-Bartrina. 1992. Reconstruction of the history of Pacific sardine and Northern anchovy populations over the past two millennia from sediments of the Santa Barbara Basin. Calif. Coop. Oceanic Fish. Invest. Rep. 33:24–40.

Becker, B. and S. R. Beissinger. in press. Centennial decline in the trophic level of an endangered seabird after fisheries collapse. Cons. Biol.

Bond, N. A., J. E. Overland, M. Spillane, and P. Stabeno. 2003. Recent shifts in the state of the North Pacific. Geophys. Res. Lett. 30:2183–2186, doi:10.1029/2003GL018597.

Brinton, E. and A. Townsend. 2003. Decadal variability in abundances of the dominant euphausiid species in southern sectors of the California Current. Deep Sea Res. II 50:2449–2472.

Charles, C. D., K. Cobb, M. D. Moore, R. G. Fairbanks. 2003. Monsoon-tropical ocean interaction in a network of coral records spanning the 20th century. Mar. Geol. 201:207–222.

Chavez, F. P., J. Ryan, S. E. Lluch-Cota, M. Niquen. 2003. From anchovies to sardines and back: Multidecadal change in the Pacific Ocean. Science 299:217–221.

Chelton, D. B., P. A. Bernal, and J. A. McGowan. 1982. Large-scale interannual physical and biological interaction in the California Current. J. Mar. Res. 40:1095–1123.

Cobb, K. M., C. D. Charles, R. L. Edwards, H. Cheng, M. Kastner. 2003. El Niño-Southern Oscillation and tropical Pacific climate during the last millennium. Nature 424:271–276.

Crowley, T. J. 2000. Causes of climate change over the past 1000 years. Science 289:270–276.

Cubasch, U. and G. A. Meehl. 2001. Projections of future climate change. *In* Houghton and others, eds. Climate Change 2001: the scientific basis. Cambridge University Press, pp. 525–582.

D'Arrigo, R., R. Wilson, C. Deser, G. Wiles, E. Cook, R. Villalba, A. Tudhope, J. Cole, and B. Linsley, 2005. Tropical-North Pacific climate linkages over the past four centuries. J. Climate 18:5253–5265.

Deser, C., A. S. Phillips, and J. W. Hurrell. 2004. Pacific interdecadal climate variability: Linkages between the tropics and North Pacific during boreal winter since 1900. J. Climate 17:3109–3124.

Di Lorenzo, E., A. J. Miller, N. Schneider, and J. C. McWilliams. 2005. The warming of the California Current: Dynamics, thermodynamics, and ecosystem implications. J. Phys. Oceanogr. 35:336–362.

Enfield, D. B. and A. M. Mestas-Nuñez. 1999. Multiscale variabilities in global sea surface temperatures and their relationships with tropospheric climate patterns. J. Climate 12:2719–2733.

Esper, J., E. R. Cook, and F. H. Schweingruber. 2002. Low-frequency signals in long tree-ring chronologies for reconstructing past temperature variability. Science 22:2250–2253.

Field, D. B. 2004a. Planktonic foraminifera in the California Current: Vertical distributions, decadal climate variability, and 20th century warming. Scripps Institution of Oceanography, UCSD. 177 pp.

Field, D. B. 2004b. Variability in vertical distributions of planktonic foraminifera in the California Current: Relationships to vertical ocean structure. Paleoceanography 19:PA2014, doi:10.1029/2003PA000970.

Field, D. B., T. R. Baumgartner, C. Charles, V. Ferriera-Bartrina, and M. D. Ohman. 2006. Planktonic foraminifera of the California Current reflect twentieth century warming. Science 311:63-66.

Field, J. C., R. C. Francis, and A. Strom. 2001. Toward a fisheries ecosystem plan for the Northern California Current. Calif. Coop. Oceanic Fish. Invest. Rep. 42:74–87.

Gargett, A. E. 1997. The optimal stability 'window': a mechanism underlying decadal fluctuations in North Pacific salmon stocks? Fish. Oceanogr. 6:109–117.

Graham, N. 1995. Simulation of recent global temperature trends. Science 267:666–671.

Graham, N. E., T. P. Barnett, R.Wilde, M. Ponater, and S. Schubert. 1994. On the roles of tropical and midlatitude SSTs in forcing interannual to interdecadal variability in the winter northern hemisphere circulation. J. Climate 7:1416–1441.

Hendy, I. L. and J. P. Kennett. 1999. Latest Quaternary North Pacific surface-water responses imply atmosphere-driven climate instability. Geology 27:291–294.

Houghton, J. T., Y. Ding, D. J. Griggs, M. Noguer, P. J. van der Linden, X. Dai, K. Maskell, and C. A. Johnson, eds. 2001. The scientific basis: Contribution of Working Group I to the Third Assessment Report of the Intergovernmental Panel on Climate Change. Cambridge University Press, pp. 525–582.

Jackson, J. B. C., M. X. Kirby, W. H. Berger, K. A. Bjorndal, L. W. Botsford, B. J. Bourque, R. H. Bradbury, R. Cooke, J. Erlandson, J. A. Estes, T. P. Hughes, S. Kidwell, C. B. Lange, H. S. Lenihan, J. M. Pandolfi, C. H. Peterson, R. S. Steneck, M. J. Tegner, and R. R. Warner. 2001. Historical overfishing and the recent collapse of coastal ecosystems. Science 297:629–637.

Kaplan, A., M. A. Cane, Y. Kushnir, A. C. Clement, M. B. Blumenthal, and B. Rajagopalan. 1998. Analyses of global sea surface temperature 1856–1991. J. Geophys. Res. 103:18,567–18,589.

Lavaniegos, B. E. and M. D. Ohman. 2003. Long-term changes in pelagic tunicates in the California Current. Deep Sea Res. II. 50:2473–2498.

Levitus, S., J. L. Antonov, T. P. Boyer, and C. Stephens. 2000. Warming of the world ocean. Science 287:2225–2229.

Levitus, S., J. L. Antonov, J. Wang, T. L. Delworth, K. W. Dixon, A. J. Broccoli. 2001. Anthropogenic warming of the earth's climate system. Science 292:267–270.

Lluch-Belda, D., R. M. Laurs, D. B. Lluch-Cota, and S. E. Lluch-Cota. 2001. Long-term trends of interannual variability in the California Current System. Calif. Coop. Oceanic Fish. Invest. Rep. 42:129–144.

Mann, M. E., R. S. Bradley, and M. K. Hughes, 1999. Northern hemisphere temperatures during the past millennium: Inferences, uncertainties, and limitations. Geophys. Res. Lett. 26:759–762.

Mantua, N. J., S. R. Hare, Y. Zhang, J. M. Wallace, and R. C. Francis. 1997. A Pacific interdecadal climate oscillation with impacts on salmon production. Bull. Amer. Meteorolog. Soc. 78:1069–1079.

McGowan, J. A., D. R. Cayan, and L. M. Dorman. 1998. Climate-ocean variability and ecosystem response in the northeast Pacific. Science 281:210–217.

Mendelssohn, R., F. B. Schwing, S. J. Bograd. 2003. Spatial structure of subsurface temperature variability in the California Current, 1950–1993. J. Geophys. Res. 108:3093–3096.

Miller, A. J., D. R. Cayan, T. P. Barnett, N. E. Graham, and J. M. Oberhuber. 1994. The 1976–77 climate shift of the Pacific Ocean. Oceanogr. 7:21–26.

Pierce, D. W. 2001. Distinguishing coupled ocean-atmosphere interactions from background noise in the North Pacific. Prog. Oceanogr. 49:331–352.

Rayner, N. A., P. Brohan, D. E. Parker, C. K. Folland, J. J. Kennedy, M. Vanicek, T. J. Ansell, and S. F. B. Tett. 2006. Improved analyses of changes and uncertainties in sea surface temperature measured in situ. since the mid-nineteenth century: The HadSST2 Dataset. J. Climate 19:446–469.

Rebstock, G. A. 2001. Long-term stability of species composition in calanoid copepods off southern California. Mar. Eco. Prog. Ser. 215:213–224.

Roemmich, D. and J. McGowan. 1995. Climatic warming and the decline of zooplankton in the California Current. Science 267:1324–1326.

Rudnick, D. I. and R. E. Davis. 2003. Red noise and regime shifts. Deep-Sea Res. 50:691–699.

Schneider, N. and B. D. Cornuelle. 2005. The forcing of the Pacific Decadal Oscillation. J. Climate 18:4355–4373.

Smith, T. M. and R. W. Reynolds. 2004. Improved Extended Reconstruction of SST (1854–1997). J. Climate 17:2466–2477.

Trenberth, K. E. and J. W. Hurrell. 1994. Decadal atmosphere-ocean variations in the Pacific. Clim. Dyn. 9:303–319.

Urban, F. E., J. E. Cole, and J. T. Overpeck. 2000. Influence of mean climate change on climate variability from a 155-year tropical Pacific coral record. Nature 407:989–993.

Venrick, E. L., J. A. McGowan, D. R. Cayan, and T. L. Hayward. 1987. Climate and chlorophyll a: Long-term trends in the central north Pacific Ocean. Science 238:70–72.

White, W. B., D. R. Cayan, and J. Lean. 1998. Global upper ocean heat storage response to radiative forcing from changing solar irradiance and increasing greenhouse gas/aerosol concentrations. J. Geophys. Res. 103:21,355–21,366.

White, W. B., J. Lean, D. R. Cayan, and M. D. Dettinger. 1997. A response of global upper ocean temperature to changing solar irradiance. J. Geophys. Res. 102:3255–3266.